Cell, Vol. 88, 39–48, January 10, 1997, Copyright ©1997 by Cell Press

Extracellular Matrix Rigidity Causes Strengthening of Integrin–Cytoskeleton Linkages

Daniel Choquet,* Dan P. Felsenfeld, and Michael P. Sheetz
Department of Cell Biology
Duke University Medical Center
Durham, North Carolina 27710

Summary

To move forward, migrating cells must generate traction forces through surface receptors bound to extracellular matrix molecules coupled to a rigid structure. We investigated whether cells sample and respond to the rigidity of the anchoring matrix. Movement of beads coated with fibronectin or an anti-integrin antibody was restrained with an optical trap on fibroblasts to mimic extracellular attachment sites of different resistance. Cells precisely sense the restraining force on fibronectin beads and respond by a localized, proportional strengthening of the cytoskeleton linkages, allowing stronger force to be exerted on the integrins. This strengthening was absent or transient with antibody beads, but restored with soluble fibronectin. Hence, ligand binding site occupancy was required. Finally, phenylarsine oxide inhibited strengthening of cytoskeletal linkages, indicating a role for dephosphorylation. Thus, the strength of integrin–cytoskeleton linkages is dependent on matrix rigidity and on its biochemical composition. Matrix rigidity may, therefore, serve as a guidance cue in a process of mechanotaxis.

Introduction

The migration of fibroblasts depends on interactions between cell-surface adhesion receptors and components of the extracellular matrix (ECM; Hynes and Lander, 1992; Lauffenburger and Horwitz, 1996). It has been suggested that cell migration results from the generation of traction forces by the cytoskeleton (CSK) at sites of cell adhesion (Harris et al., 1981; Sheetz, 1994; Lauffenburger and Horwitz, 1996; Mitchison and Cramer, 1996). Traction forces have indeed been experimentally observed and measured (Harris et al., 1981; Lee et al., 1994; Oliver et al., 1995). They can deform collagen gels or compliant substrata, leading to rearrangement of collagen fibrils in vivo (Stopak et al., 1985), or govern cell shape (Sims et al., 1992). Furthermore, they can be regulated by tyrosine phosphorylation (Crowley and Horwitz, 1995). Force generation is made possible by the ability of adhesion receptors such as integrins to bind simultaneously to matrix components through their extracellular domains, and to CSK elements through their cytoplasmic domains. Thus, these adhesion receptors transmit the mechanical tension generated within the CSK as the migrating cell pulls itself forward.

For the force generated by the cell to result in net cell movement, the adhesion site must be associated with a rigid structure in the ECM. Therefore, it is important to know whether the cell can sample the resistance of an anchoring site and detect, for example, that free aggregates of matrix molecules are different from the same molecules assembled into a rigid network. One possible difference between free and bound matrix molecules is the physical force with which bound molecules can resist forces applied by migrating cells.

Previous work has shown that whole cells can increase their rigidity in response to physical stress (Sato et al., 1987; Zhelev and Hochmuth, 1995) and that CSK assembly and matrix organization on the cell surface is influenced by matrix stiffness (Halliday and Tomasek, 1995). More specifically, the use of integrin ligand–coated beads showed that CSK stiffness increases in proportion to stress applied to integrins (Wang et al., 1993; Wang and Ingber, 1994). Although structural rearrangements within an interconnected CSK lattice could occur, the cell may alternatively locally control the formation of adhesion sites as a function of the resistance of localized cell–substrate attachments.

Fibronectin is a major ECM component used by many cell types as a substrate for attachment and migration (Ruoslahti, 1988). The most common fibronectin receptor is the $\alpha5\beta1$ integrin (Dalton et al., 1992). Fibronectin binds to the integrin in fibroblasts through a consensus site including the Arg-Gly-Asp (RGD) sequence (Ruoslahti, 1988). Unbound integrins are freely diffusive in the membrane plane (Duband et al., 1988; Schmidt et al., 1993; Felsenfeld et al., 1996). Aggregation and ligand binding promote redistribution of integrins to focal adhesion contacts and attachment to rearward-moving CSK (Duband et al., 1988; LaFlamme et al., 1992; Schmidt et al., 1993; Miyamoto et al., 1995; Felsenfeld et al., 1996), in a mechanism that may involve the tyrosine kinase FAK (for focal adhesion kinase; Romer et al., 1992) and that occurs through the $\beta1$ cytoplasmic tail (Reszka et al., 1992).

It remains unknown whether the degree of tension in the ECM is also a local determinant of the adhesion site characteristics. Thus, we wished to analyze whether there exists a feedback mechanism allowing the cell to adjust traction forces it exerts as a function of anchoring site resistance. This is analogous to asking whether cells can function similarly to muscles matching contractile force to the load.

To apply loads on spatially defined sites of attachment and estimate the traction forces exerted by the cell, we used latex beads coated with ligand as a surrogate for ECM binding sites. Such beads direct the formation of focal contact like aggregates of CSK elements (Wang et al., 1993; Miyamoto et al., 1995). We used an optical gradient trap to place the beads on the cells and apply calibrated forces (Ashkin, 1992; Kuo and Sheetz, 1992). Freely moving, cell surface–bound, fibronectin-coated, or anti-$\beta1$ antibody–coated beads were used to mimic

*Present address: UMR CNRS 5541, Université Bordeaux 2, 146, rue Leo Saignat, 33076 Bordeaux Cedex, France.

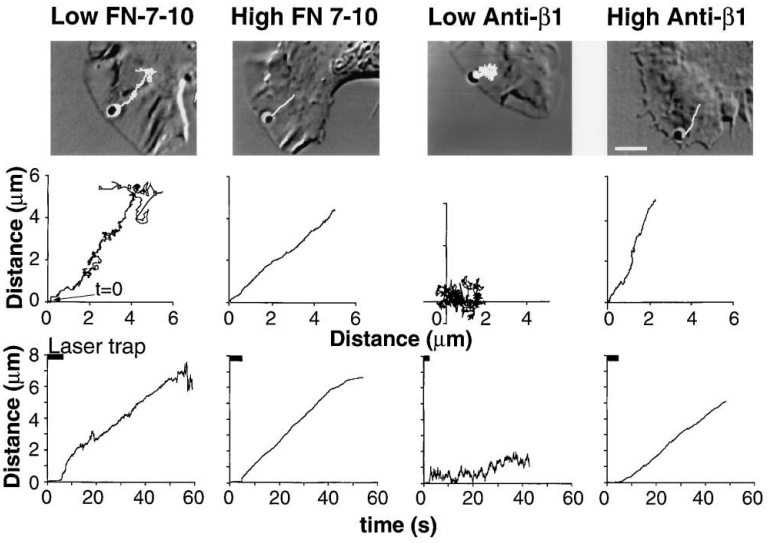

Figure 1. FN7-10- and High Density anti-β1-Coated Beads Move Rearward on Lamellipodia of Fibroblasts

(Top) Differential interference contrast (DIC) images of the lamellipodia of motile NIH 3T3 fibroblasts at the time at which 1-μm latex beads have been placed on the cell surface with the laser tweezers. The beads were coated respectively with the FN7-10 recombinant fragment of fibronectin at low (left) and high (middle left) concentration, and with a nonactivating anti-β1 antibody at low (middle right) and high (right) concentration (see Experimental Procedures). The trajectory of the bead in the first 40–60 s after contacting the cell is superimposed as a white line. Scale bar, 5 μm.

(Middle) X–Y plots of bead movement for 40–60 s after initial bead–cell contact (at the origin of the plot) for the beads shown in (A). X axis is horizontal, oriented left–right from the micrographs; Y axis is vertical, oriented bottom–top. At the end of its movement, the low FN7-10-coated bead detached from the cell surface (left), while the high FN7-10- and antibody-coated beads remained attached for the whole length of the experiment. Only the low anti-β1-coated bead purely diffused in the plane of the membrane and did not display rearward directed movement.

(Bottom) Plots of bead displacement from the leading edge versus time with reference to the point and time at which the bead initially came into contact with the lamellipodia. Traces are from the same experiments as in (A) and (B) in which the trap was turned off 1–4 s after initial bead–cell contact. The period during which the trap is on is indicated by the thick line on top of both graphs.

the behavior of integrins bound to a flexible substrate or free aggregates of matrix molecules. Bead movement was then restrained with the optical trap to model integrin attachment to a more rigid site in the ECM.

Results

FN7-10- and Anti-β1 Antibody–Coated Beads Are Transported Rearward on the Cell Surface

To observe the behavior of the α5β1 integrin in the presence or absence of bound ligand, we prepared 1-μm beads coated at different densities either with a nonactivating anti-chicken β1 antibody (Duband et al., 1988) or with a recombinant fragment of fibronectin, including the type III repeat 7–10 domains (FN7-10; Leahy et al., 1996). This 40-kDa peptide contains the α5β1 integrin–binding domain (Kimizuka et al., 1991) but lacks other domains that might interact with other receptors. Experiments were carried out on mouse NIH 3T3 fibroblasts expressing normal or mutant forms of the chicken β1 integrin (Solowska et al., 1989; Schmidt et al., 1993).

When FN7-10-coated beads were held on the lamellipodia of fibroblasts expressing normal chick β1 with laser tweezers for 1–7 s, they bound and moved rearward toward the nucleus at a speed of 5–10 μm/min (Figure 1), independent of the density of FN7-10 we used on the bead (≈50–5000 molecules/μm^2). In contrast, the movement of anti-chick β1–coated beads on the cell surface was strongly dependent on the ligand density. Of the low density anti-β1 beads (incubated with 5 μg/ml antibody) that bound to the cell (n = 20 out of 39 beads), 90% displayed a purely diffusive movement (n = 20). At high antibody density (500 μg/ml), most beads bound to the cell (n = 32 out of 36 beads), and 50% displayed a clear directed movement (n = 32), similar to that of FN7-10-coated beads; the rest diffused freely in the membrane plane.

Directed bead movement paralleled that of rearward-moving CSK material (data not shown). Furthermore, the speed of rearward movement did not appear to depend on the type of ligand (fibronectin or antibody) or its density on the bead. Speed ranged between 0.08 μm/s and 0.23 μm/s (average 0.11 ± 0.03 μm/s, n = 50 FN7-10 beads; 0.10 ± 0.04 μm/s, n = 17 antibody beads; all data mean ± SD; see also Table 1). These values are within the published velocities of rearward-moving actin CSK (Forscher and Smith, 1988; Theriot and Mitchison, 1991), suggesting that in these cells the retrograde movement of receptors is driven by the rearward flow of actin (Dembo and Harris, 1981; Kucik et al., 1991; Lin and Forscher, 1995).

In contrast, bead binding to the cell as well as the random diffusion component of bead movement displayed a strong dependence on the density and type of ligand on the bead. The percentage of beads binding to the cell decreased with ligand density (see above; Figure 2B). More importantly, low density anti-β1 beads diffused freely in the membrane, probably revealing the behavior of unliganded integrins (Felsenfeld et al., 1996). By contrast, high density anti-β1 beads and all densities of FN7-10 beads actively moved toward the nucleus, further demonstrating that cross-linking of integrins with anti-β1 antibodies also produces engagement with the CSK. It remains to be determined whether cross-linking of fibronectin-bound integrins is a requirement for attachment to the CSK.

Our data also suggest that the degree of attachment to the CSK depends on FN7-10 density on the beads. Although most FN7-10 beads displayed rearward movement (Figures 1 and 2), the diffusive component displayed a strong dependence on ligand density. At the

Table 1. Diffusion Coefficient and Velocity of Beads with or without Restraint

	Diffusion (10^{-10} cm^2/s)			Velocity (μm/s)		
Bead Movement	Low FN7-10	High FN7-10	Anti-β1	Low FN7-10	High FN7-10	Anti-β1
Freely moving beads	0.546 ± 0.620 (13)	0.064 ± 0.080 (17)	2.063 ± 3.170 (6)	0.121 ± 0.038 (13)	0.107 ± 0.027 (17)	0.078 ± 0.020 (6)
Restrained beads	0.032 ± 0.010 (9)	0.014 ± 0.007 (11)	0.112 ± 0.200 (11)	0.111 ± 0.014 (9)	0.117 ± 0.034 (11)	0.112 ± 0.046 (11)

Left, diffusion coefficients for the indicated ligands on the beads (mean ± SD) during rearward movement for freely moving beads (i.e., beads held <2 s in the trap and then let free) or for restrained beads after escape. Beads displaying a purely diffusive behavior were excluded. The diffusion coefficient for a stationary bead held in a laser trap was 0.004×10^{-10} cm^2/s. At low and high FN7-10 levels, the differences between free and restrained beads were significant ($p < 0.025$). The differences between free high and free low, between restrained high and restrained low, between restrained high and restrained anti-β1, were significant ($p < 0.01$).
Right, mean and standard deviation of the bead velocity in the same conditions as shown on the left. Only the velocity of free anti-β1 beads was significantly different from the others ($p < 0.03$).
The number of beads measured in each case is shown in parentheses.

highest FN density, the diffusion coefficient, D, was as low as 0.007×10^{-10} cm^2/s (average $D = 0.064 \times 10^{-10} \pm 0.0084 \times 10^{-10}$ cm^2/s, n = 17; see also Table 1), consistent with a tight attachment to CSK elements. At low densities, D ranged from 9.30×10^{-10} cm^2/s for the few freely diffusing beads to 0.033×10^{-10} cm^2/s for beads displaying rearward movement (average $D = 1.98 \times 10^{-10} \pm 2.78 \times 10^{-10}$ cm^2/s, n = 20, significantly higher than that of high density beads $p < 0.01$). As a control experiment, we used fibroblasts expressing a truncated β1 subunit (Solowska et al., 1989) lacking the cytoplasmic tail. Out of 13 high density antibody–coated beads placed on these cells, 12 displayed a purely diffusive behavior (data not shown), while one moved rearward.

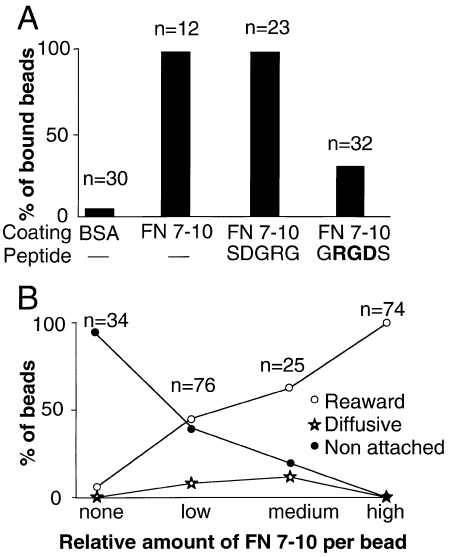

Figure 2. Specificity and Dose Dependence of FN7-10-Coated Bead Binding to Fibronectin Receptors

(A) Histogram of the percentage of beads that bound to the cell as a function of coating and presence of soluble peptide. In these experiments, the binding of beads coated with BSA or recombinant FN7-10 fragment of fibronectin was assessed on lamellipodia of motile cells by holding the beads for 4 s on the cell surface with the tweezers and then releasing the trap. Unbound beads drifted out of focus into the extracellular medium within seconds. Bead binding was inhibited in the presence of 1 mg/ml of the fibronectin receptor agonist peptide GRGDS, but not the same concentration of the control scrambled peptide SDGRG. The total number of beads tested in each condition is given above each bar. $p < 0.001$ that behavior of BSA beads or FN7-10 beads in the presence of GRGDS are similar to control FN7-10 beads, χ^2 test.

(B) Plots of the percentage of beads displaying no binding (closed circle), diffusive movement (star), or rearward-directed movement (open circle) as a function of the relative concentration of FN7-10 on the bead surface. The amount of FN7-10 per bead was varied as indicated in Experimental Procedures. The total number of beads tested in each condition is given above each category. $p < 0.15$ that low and medium FN7-10 densities come from the same population, comparing bound and unbound beads. $p < 0.001$ that all other density categories compared one with the other come from the same population.

Finally, at low FN7-10 density, 21 out of 43 beads eventually unbound from the cell. Unbinding seemed to occur preferentially at the rear of the lamellipodia, near the endoplasm–ectoplasm boundary. Antibody-coated beads did not release from the cell surface.

To ascertain the specificity of binding, beads were coated with bovine serum albumin (BSA), displaying marginal binding (6%, n = 30) and no attachment to the CSK. FN7-10 bead binding was blocked by the addition of GRGDS peptide (1 mg/ml) but not scrambled peptide SDGRG (1 mg/ml) (Figure 2). Thus, beads attach to the RGD-sensitive receptor, $\alpha5\beta1$, present in these cells (Dalton et al., 1992). Unless mentioned, all further experiments were carried out with high density FN7-10 beads.

In summary, both FN7-10 and antibody-coated beads bind specifically to integrins promoting their attachment to the rearward moving CSK. However, FN7-10 beads bind more readily to the CSK, and the degree of anchoring, evidenced by the diffusive coefficient of movement, is proportional to the density of ligand on the bead.

FN7-10- but Not Antibody-Coated Beads Display Reinforcement of the Links to the CSK upon Application of a Restraining Force to the Bead

We next determined the strength of the linkage to the CSK after initial bead–cell contact as a function of the extent of restraint of bead freedom of movement and type of ligand on the bead. After a bead was placed on the lamella, a second application of the trap force was used to pull the bead back toward the leading edge after it had traveled toward the nucleus (Figure 3A, inset). This was performed by repositioning the stage so that the bead center was 0.5–0.7 μm ahead of the trap center (about the point of maximal trap force; see below), with respect to the bead path. The trap was then turned

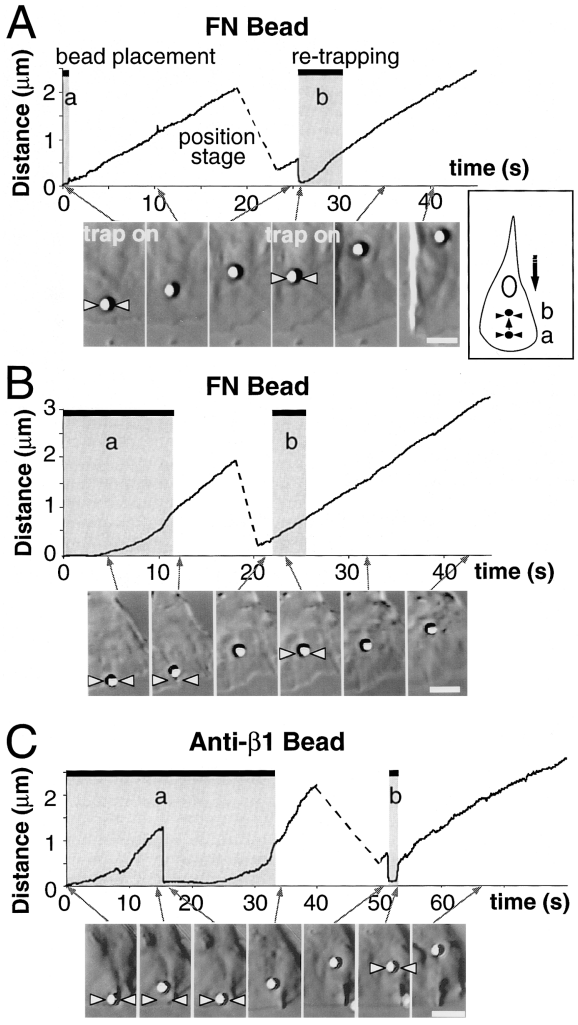

Figure 3. FN7-10- and Not Anti-β1-Coated Beads Display Increased Stiffness of Links to the CSK after Application of a Force Restraining Bead Movement

(A, B, and C, top, traces) Plots of bead displacement from the leading edge versus time with reference to the point and time at which the bead initially came into contact with the lamellipodia. Beads were respectively coated with FN7-10 (A, B) or anti-β1 (C). Traces are from three separate experiments in which (A) the trap was turned off 1.5 s after initial bead–cell contact, or (B, C) the trap remained on (shaded area labeled [a]) until the bead escaped its radius of action (about 2.0 μm away from its center, which is always at distance 0), that is, respectively, for 12 s and 34 s in (B) and (C). After the beads traveled over 2 μm, the stage was moved (broken line) to reposition the bead within 0.7 μm of the trap center (the latter being placed behind the bead, with respect to its direction of movement). The laser was then turned on again to apply force on the bead to assess the strength of the bead–CSK link (shaded area labeled [b]). This protocol is illustrated in the inset in (A). With the brief initial trap exposure (A, [a]) the retrapping immediately moved the bead back toward the trap center, but the bead resumed its forward movement within seconds despite the continuous presence of the trap. In contrast, after first experiencing escape from the maximum trap force (B, [a]; C, [a]), retrapping did not move the FN7-10-coated bead (B, [b]), but could move the antibody-coated one (C, [b]). Note that during (C, [a]), there was a spontaneous breakage of the CSK links, leading to a pop back of the bead toward the trap center. Laser intensities used in these experiments generated maximum trap forces of 10–20 pN.

(A, B, and C, bottom, images) Sequential DIC images of the cell regions through which the bead traveled during the course of the experiment represented in (A), (B), and (C) (top traces). The position of the focal point of the laser trap is represented by the two arrowheads. Scale bar, 2 μm.

on, and bead displacement was measured by single-particle tracking of video frames (Gelles et al., 1988). As shown in Figure 3A, beads that were held initially (labeled [a] in the figure) in the laser tweezers for only 0.5–2.0 s could be moved (labeled [b]) with forces in excess of 5 pN irrespective of FN7-10 density (79%; n = 34 beads moved >100 nm). No membrane deformation was evident, indicating that bead rolling on the surface is not the primary means of movement.

When a restraining force of more than 10 s duration was applied to the bead during initial contact, beads stalled, but then moved rearward, rapidly escaping the force field of the trap (Figure 3B, label [a]). The field is maximal at about 0.5 μm from the center of the trap (Simmons et al., 1996) and decreases until about 2 μm, where it is less than Brownian forces. At high FN7-10 densities, 100% of the beads escaped the maximal tweezers force. However, at low FN7-10 densities, only 15 out of 39 of the bound beads escaped the tweezers (set at forces of 8–15 pN), showing that the maximum linkage strength was dependent upon the FN7-10 density. Strikingly, when the cell pulled the bead out of the trap (Figure 3B, label [a]), the same or a lower force could not move the bead (Figure 3B, label [b]). We defined this process as reinforcement of the linkage of a bead to the cell, characterized by a decrease in the ability of a given optical trap force to displace the bead on the cell surface. This reinforcement was systematically observed for restraining forces ranging from 5 pN to 60 pN on 81 out of 90 beads.

Reinforcement was not observed with anti-β1-coated beads. As shown in Figure 3C, an antibody-coated bead traveled for about 1 μm and popped back to the trap center, implying that the CSK link spontaneously broke (Figure 3C during label [a]). This rupture occurred past the point of maximum force (≈0.5 μm), suggesting a weakening of the CSK linkage. This bead eventually fully escaped the tweezers, but when the strength of the CSK links was later assayed (Figure 3C [b]), the links were weak enough to allow bead displacement by the tweezers. After the trap is turned off (b), the bead pops back to its original position, indicative of the elasticity of CSK links.

Diffusion coefficient was used as another measure of the rigidity of the bead attachment to the CSK. The diffusive component was decreased after the bead escaped the laser trap (Table 1). This effect was most dramatic on low density FN7-10 beads, whose diffusion coefficient was 17 times lower for reinforced beads than for unrestrained ones. High density beads displayed a 5-fold decrease. In contrast, antibody-coated beads did not exhibit a statistically significant decrease after they escaped the trap.

Taken together, the decrease in bead diffusion coefficient and the decrease in movement in response to an applied force indicate that restraining the rearward movement of FN7-10-coated beads on the cell surface

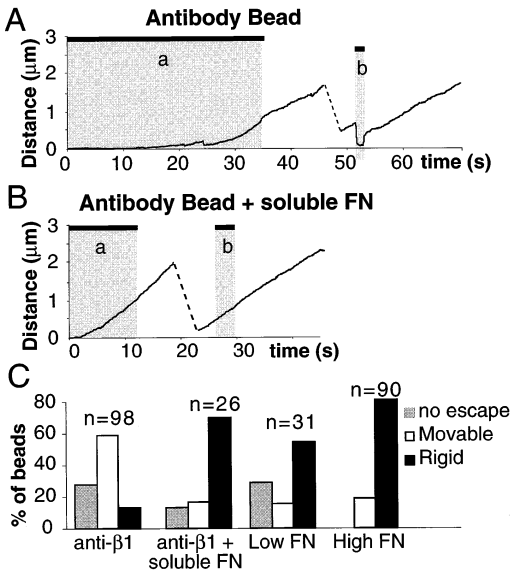

Figure 4. Anti-β1-Coated Beads Display Reinforcement of CSK Links in the Presence of Soluble FN7-10

(A, B) Plots of displacement versus time of anti-β1-coated beads in the absence (A) and presence (B) of 20 μg/ml soluble FN7-10. Beads were positioned with the tweezers on the lamellipodia near the leading edge at time 0, and the trap remained on for the time indicated by the shaded area (a), until the beads escaped the trap. The rigidity of bead attachment to the cell was then assessed by repositioning the trap 0.5 μm behind the bead (broken trace). The trap was turned on during the period labeled (b), and the movement of the bead in response to the applied force was measured. The trap force was 18 pN in this experiment, and both beads were recorded on the same dish of cells, both before and 5 min after the addition of soluble FN7-10, respectively.

(C) Histogram of the percentage of beads displaying reinforcement of CSK links as a function of bead coating and presence of soluble FN7-10. All beads were subjected to a restraining force after initial bead–cell contact until they escaped the trap. If no escape was observed after 15–20 s, trapping was discontinued and the bead scored accordingly (gray bars). For beads that did escape, the strength of CSK links was assayed as in Figures 3–6 and beads scored as movable (open bars) or rigid (closed bars), whether the trap force could or could not displace the bead. The total number of beads tested in each condition is given above each bar group. All distributions were significantly different one from the other ($p < 0.005$), except between anti-β1 beads with soluble FN7-10 and low density FN7-10 ($p > 0.1$).

induces an increase in the strength and rigidity of the linkages to the CSK. This is not observed with anti-β1-coated beads.

Antibody-Coated Beads Display Reinforcement in the Presence of Soluble FN7-10

The inability of anti-β1-coated beads to display reinforcement prompted us to investigate whether occupation of the integrin ligand–binding site, rather than integrin aggregation alone, was required for reinforcement. In the presence of soluble FN7-10 fragment (20 μg/ml), anti-β1-coated beads behaved similarly to FN7-10-coated beads (Figure 4). Of anti-β1-coated beads with soluble FN7-10, 80% displayed reinforcement of CSK links ($n = 26$), as opposed to only 17% for control anti-β1 beads ($n = 17$). Anti-β1-coated beads with soluble FN7-10 escaped from the trap at times comparable to that of FN7-10-coated beads (11.7 ± 4.1 s, $n = 14$, to travel 0.5 μm from the trap center), about three times faster than control anti-β1-coated beads (27 ± 8.7 s, $n = 11$, $p < 0.0001$). This difference is not due to soluble FN7-10 binding to the beads, since protein-binding sites on the beads were blocked with BSA.

Together (Figure 4C), these data establish that occupancy of the fibronectin-binding sites on the integrin, and not primarily the degree of integrin cross-linking, is required for reinforcement.

Reinforcement Is Proportional to Restraining Force and Occurs within Seconds

The strengthening of integrin–CSK linkage was graded; 88% ($n = 33$) of FN7-10 beads that escaped from a given tweezers force could be moved by a 10-fold higher force (Figure 5A). To determine more precisely the magnitude of force needed to deform a bond reinforced by a given load, we titrated the amount of force required to move a bead after it escaped a given trap force (Figure 5B). On average, beads could be moved by a force three times higher than the initial restraining force.

To determine the time course of reinforcement as a function of tweezers force, we followed the movement of beads escaping from traps of increasing strengths. In all cases, the steady-state velocity of 6–10 μm/min was reached after 5–10 s. This pattern of movement was independent of the strength of the tweezers (for peak forces of 3 pN to 50 pN, see Figures 5B and 5C). The force of the tweezers is maximal at a distance from the trap center of one bead radius, i.e., 0.5 μm (Ashkin, 1992) (see mark in Figure 5C). Even at the highest laser intensity, the point of maximal force was attained within 10 s.

Further insight into the time course of reinforcement and differences between antibody- and FN7-10-coated beads comes from the analysis of spontaneous release from the CSK. Both antibody-coated and low density FN7-10 beads exhibited occasional spontaneous pops back toward the trap center (see Figure 3C). A similar phenomenon had previously been observed for conA-coated beads (Kucik et al., 1991). However, while release for FN7-10 beads mostly occurred within 0.5 μm of the trap center, release for antibody beads could occur as far as 1.5 μm from the trap center, where the force is only a small fraction of the maximum. This suggests that the CSK links with antibody beads are reversible; with low density FN7-10 beads, the links are weak enough to be broken by the trap. Together, these experiments suggest that strengthening of linkages under the bead occurs during the first seconds of escape from the trap and closely matches the restraining force.

Reinforcement Is Localized

In a variety of systems, there is a general cell activation that results from localized external ligand binding. We therefore explored the spatial resolution of the reinforcement by testing for the effect of reinforcing one bead on the level of reinforcement of a neighboring bead (both bead centers separated by about 2 μm). We never saw any cross-talk between the level of attachment of two

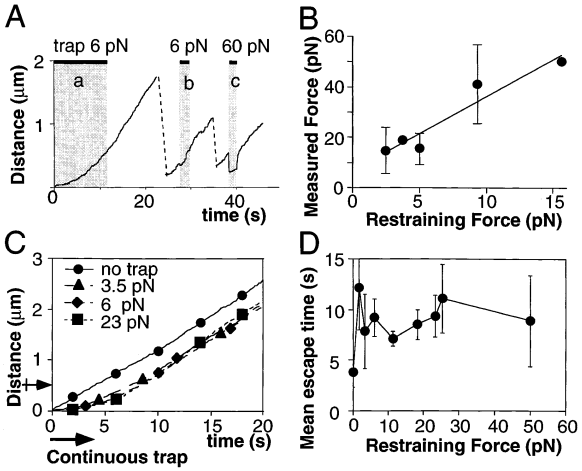

Figure 5. The Amount of Reinforcement of CSK Links Is Proportional to the Applied Restraining Force

(A) Displacement versus time of a FN7-10-coated bead that initially escaped a 6 pN force and whose strength of CSK attachment was further tested with a 6 pN and a 60 pN trap. Only the latter could move the bead.

(B) Plot of the amount of force required to move beads (ordinate) that have escaped a given restraining trap force (abscissa). Each FN7-10-coated bead was allowed to escape from a trap of given force and then successively assessed for the ability to be displaced by traps of increasing forces in 2-fold increments. This was performed by placing the trap center roughly 0.5 μm away from the bead center and switching the laser on, repeating this procedure with increasing force on the same bead. A force was scored as able to displace the bead if the latter moved by more than 100 nm. These measured forces were averaged for all beads restrained by a given force (a minimum of six beads was tested at each restraining force). For a restraining force of 15 pN, 3 out of 6 beads could not be displaced even by the highest force (50 pN). Data are given ± SD and fitted with a linear regression line of slope 2.9 and correlation coefficient of 0.96.

(C) Superimposed traces of trajectories of beads during escape from laser traps having a maximal force of 3.5, 6, and 23 pN. Each trace corresponds to one laser power and is the mean of four to seven individual bead traces. Each bead was put into contact with the cell at time zero and the tweezers left on until the bead had moved 1 μm. For comparison, the mean trajectory of beads that did not experience force is included (closed circle). Note that these beads move at a constant speed just after contacting the cell. All experiments were performed on the same batch of cells.

(D) Mean time and SD for beads to move 0.5 μm from the trap center versus maximum trap force for the same experiments as in (C).

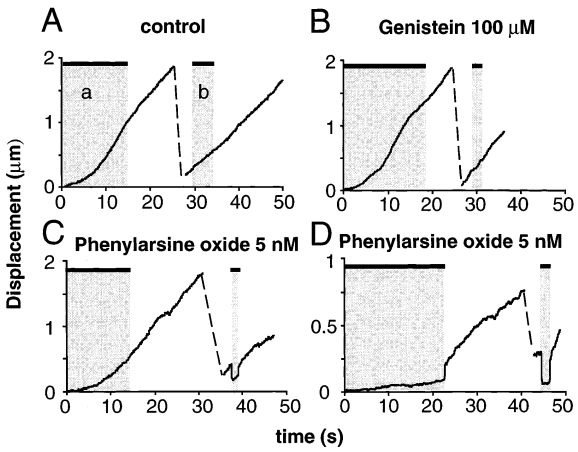

Figure 6. Inhibition of Resistance-Induced Reinforcement of Bead–CSK Links by PAO

Bead displacement versus time during a 15–20 s application of 25–30 pN restraining force after initial cell–bead contact (label [a]) and subsequent test for strength of the bead attachment (label [b]). In control conditions (A) and in the presence of 100 μM genistein (B), reinforcement of bead–CSK attachments by force is observed. In the presence of 5 nM PAO, beads either display no reinforcement (C) or cannot escape the trap (D).

neighboring beads (n = 6 pairs). When one of the beads was restrained by the tweezers and displayed reinforcement, the other one never displayed reinforcement. Reinforcement is therefore limited to a maximum area of 8–12 μm^2 around the bead center.

Restraining Force and Not Laser Irradiation Causes Reinforcement

Since laser tweezers force was proportional to the laser light intensity, reinforcement correlated with both laser irradiation dosage and the applied restraining force. Thus, it remained plausible that reinforcement was caused by a byproduct of laser irradiation, rather than by the applied restraining force itself. To determine whether photodamage caused reinforcement, we developed a tracking system that allowed irradiation of a bead during rearward movement without applying force. A feedback circuit using position information from a quadrant detector (Finer et al., 1994) drove a piezoelectric stage to hold the bead within 50 nm of the trap center, where it experienced <10% of the maximal force (Ashkin, 1992). Beads irradiated with a laser light for 20 s while moving rearward without restraint could then be moved toward the leading edge with a trapping force generated by the same laser power (n = 28 out of 38 beads; forces 18 pN to 50 pN; data not shown), indicating that the CSK linkage was not reinforced. The displacement of these beads was indistinguishable from that of beads that were not irradiated. This demonstrates that application of force, and not laser irradiation, induces reinforcement.

A Biochemical Step Is Involved in Reinforcement

Finally, we tried to determine whether phosphorylation was involved in reinforcement by adding kinase and phosphatase inhibitors. Low doses of the tyrosine phosphatase inhibitor phenylarsine oxide (PAO) could block this process specifically (Figure 6), with no effects on lamellipodia morphology and rearward CSK movement as demonstrated by the normal speed of rearward bead movement. In the presence of PAO, beads either could not escape the trap within 10 s (13 out of 34), or if they escaped the trap, they could still be displaced by the same force (17 out of 21). This suggests that reinforcement is rapidly reversible after escape from the trap. In contrast, a high dose of the tyrosine kinase inhibitor genistein had no effect on bead reinforcement (nor did the protein kinase C activator, phorbol myristate acetate [PMA]). A number of other drugs blocked both cell motility and attachment to CSK, and no dose could discriminate the two (e.g., another tyrosine phosphatase inhibitor, vanadate; buffering intracellular calcium with a

calcium chelator inhibited motility in general). PAO is unusual in its ability to block selectively the strengthening of adhesive contacts without blocking the process of rearward migration.

Discussion

Specificity and Ligand Dependence of the Reinforcement of Integrin–CSK Links by Load

In these studies, we have observed that the cell response to unrestrained FN7-10-coated beads is different than that to beads that are restrained with the laser tweezers. The rearward transport of bound objects such as the FN7-10 beads is a robust process on lamellipodia in motile fibroblasts. Thus, the cell will naturally exert a force on beads by moving them from the trap center. In the act of moving the FN7-10 bead against a force, the cell creates a stronger linkage between the CSK and the FN7-10-bound integrin. The maximum strength of the linkage is dependent on the tweezers force as well as the density of FN7-10 per bead. This suggests that the cell can sense the restraint as well as the number of bound FN7-10 molecules in an adhesive site. Reinforcement is rapid, restricted to the bead that experiences the force, and stable over the course of travel of the bead.

Although sufficient aggregation with a nonactivating antibody can also induce binding of integrins to rearward-moving CSK (Schmidt et al., 1993; Figure 1), load-dependent reinforcement of cross-linked integrins was absent or transient. In contrast, addition of a soluble integrin ligand allowed antibody-coated beads to display a reinforcement behavior similar to that of FN7-10-coated beads. These results establish that load-dependent reinforcement of integrin attachment to the CSK depends on occupancy of the integrin ligand–binding site by FN7-10.

One of the surprising aspects of the reinforcement process was the reversibility of attachments to the CSK with beads bound by anti-integrin antibodies or FN7-10-coated beads in the presence of PAO. They could resume more rapid diffusion seconds after escaping from the trap and showed no reinforcement. Thus, phosphorylation may be involved in reversal of integrin–CSK attachments.

Parameters Involved in the Reinforcement of CSK Linkages

It has been widely reported (e.g., Lotz et al., 1989) that upon plating of cells on fibronectin or other substrates, there is a time-dependent increase in adhesion. This is best explained by a concomitant increase in cell–substrate contact area and associated establishment of new bonds with the substrate and is likely to be different from the acute control of force described here. Previous experiments on endothelial cells using integrin ligand–coated magnetic beads to apply stresses on adhesion sites have indicated an increase in CSK stiffness proportional to the applied strain, which might be related to the reinforcement process that we describe (Wang et al., 1993; Wang and Ingber, 1994). The linear stiffness versus strain relationship was interpreted in terms of a global modification of the interconnected CSK lattice. In our experiments, the reinforcement of attachments is extremely restricted in space. However, attachments remained reinforced over the whole period of travel of the bead, often a distance of over 10 μm. These results indicate that, in our case, rigidification of CSK links occurs only under the restrained bead and does not extend to beads 1.5–2.0 microns away.

The bead movement toward the cell nucleus is probably due to the anchoring of the integrins to rearward-moving actin (Dembo and Harris, 1981; Forscher and Smith, 1988; Kucik et al., 1991; Lin and Forscher, 1995; Theriot and Mitchison, 1991). These bead–CSK attachments display a partially elastic behavior, since after retrapping and subsequent release, the beads can bounce back to their original position (for example, see Figures 4C and 5A). This shows that when normal cell-powered bead movement is impaired by an external force, a significant tension is generated in the CSK. Our data demonstrate that, in the process of reinforcement, there is a dramatic increase in the stiffness of the CSK–FN7-10 link, leading to an increase in the force exerted by the cell on the site of contact. Experiments in which the bead–cell link breaks and is subsequently reinforced, permitting the bead to pull free of the trap, further indicate that there is an increase in the total strength of the link, in addition to stiffening.

Mechanisms for the Regulation of the Strength of CSK Linkages

A number of models can explain the increase in attachment strength during application of a restraining force (Figure 7). Additional components in the CSK–FN7-10 linkage may passively accumulate as the site of contact is immobilized with respect to the rearward flow of CSK elements. However, this mechanism implies a strong temporal dependence of the reinforcement process. The time taken by the beads to escape the trap is independent of force (Figure 5), while the response of the cell is proportional to the applied force. This precludes any model based on time alone. Particularly, the addition of integrins to the contact site would have to be an active process to explain the absence of time dependence. Recruitment of integrins is unlikely, since unliganded integrins diffuse freely in the membrane (Duband et al., 1988; Schmidt et al., 1993; Felsenfeld et al., 1996), and liganded integrins would not be available for interaction with the bead. Second, antibody-coated beads do not display stable reinforcement, although they are coupled to the CSK and, on average, take longer to escape the trap. Finally, a phosphatase antagonist inhibits strengthening, pointing to the involvement of an enzymatic cascade. We thus favor the involvement of an active biochemical process.

The mechanism of reinforcement may be separated into two phases, an onset and a stabilization phase, as indicated by the behavior of antibody-coated beads and FN7-10-coated beads in the presence of PAO. The ability of some antibody-coated beads to escape the laser trap indicates that there can be a transient reinforcement of the linkages (onset phase). However, reinforcement

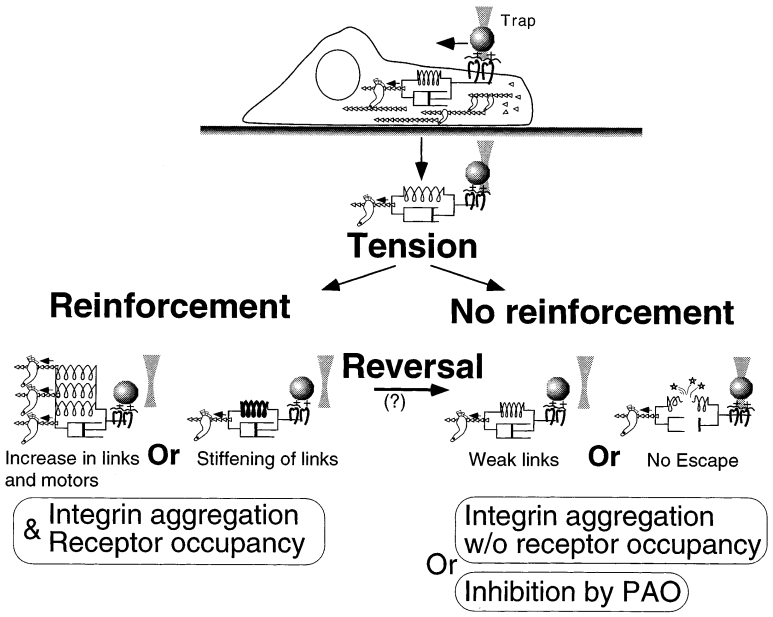

Figure 7. Model of the Regulation of FN7-10–CSK Linkages as a Function of ECM Resistance to Displacement

Binding of FN7-10 and cross-linking of integrins induces their attachment to the rearward moving CSK. Linkage to the CSK is modeled as a spring element in parallel with viscous drag. Movement is powered by a force (small arrow). As the bead movement is restrained by the laser trap, CSK linkages are put under tension. Stronger integrin–CSK links are formed when the CSK overcomes the trap force to move the particle rearward (bottom left, reinforcement) with FN7-10 beads or with anti-β1 beads in the presence of soluble FN7-10. This could occur either by strengthening of existing links or by recruitment of additional links and associated motor elements. There is no reinforcement with anti-β1 beads, or with FN7-10 beads in the presence of the phosphatase inhibitor PAO (bottom right, no reinforcement). In some cases, these beads can escape the trap but then display weak links, suggesting that there can be a reversal of the stiffening of links. The linkage breaks and the bead does not escape the trap when the resistance of the link is too weak to overcome the trap force.

is reversed within tens of seconds. Similarly, there is a transient reinforcement with FN7-10-coated beads in the presence of PAO. This argues for the involvement of a protein phosphatase in the stabilization phase of reinforced links.

In building working models, one must distinguish the sensing mechanism that detects the traction force on an attachment point and the effector system that reinforces the attachment. The rearward flow of actin may be powered by myosins (Lin et al., 1996), but in some systems that flow is clearly independent of bipolar myosin (Wessels et al., 1988). A mechano enzyme could be part of the link between the integrins and the CSK. Its activation would be triggered as the site of contact with the ECM is put under tension and would result in biochemical modification or recruitment of new CSK elements leading to rigidification of the links, for example by allowing for the coupling of new cross-linking elements.

Alternatively, we favor a model in which local deformations in the CSK matrix could concentrate CSK-associated enzymes to the contact site that would reinforce the contact by proximity-dependent modifications, addition of new elements, or both. Reinforcement can then occur by biochemical stabilization of inter-CSK protein links. The antibody experiments show that binding of integrins to the CSK is not enough to trigger this mechanism. We further suggest that activation of the integrin by FN7-10 stimulates an enzyme, such as a phosphatase, participating in the stabilization of the linkages.

Implications for the Guidance of Cell Movement by Extracellular Matrix Rigidity: Is Mechanotaxis a Possible Guidance Mechanism?

At the cellular level, there are many potential advantages to sensing the resistance of the matrix. By regulating forces at individual sites in response to the resistance of the extracellular environment, the cell could navigate as a function of the elastic properties of the underlying substrate. Previous studies have shown that cells can sense and respond to applied forces (Sato et al., 1987; Wang et al., 1993; Wang and Ingber, 1994; Zhelev and Hochmuth, 1995). Along this line, the organization of actin bundles within the cell is favored by rigid versus relaxed substrates (Shirinsky et al., 1989; Halliday and Tomasek, 1995). Furthermore, it has been recently observed that neutrophils moving in three-dimensional matrices chose to move along the most rigid fibrils after probing the environment (Mandeville et al., 1996). In our case, we find additionally that the cell can develop a force on fibronectin contacts in proportion to the resistance of those contacts. When the matrix resists movement, the linkage to the CSK is strengthened, enabling the cell to pull itself forward or to generate a traction in the matrix. Biochemical processes responsible for that strengthening can be modulated, affording the cell control mechanisms for both assembling and disassembling linkages to the CSK as the force on those linkages changes. Thus, the cell can readily sample and respond to the physical as well as the biochemical nature of its extracellular contacts.

Most models for substrate-based cell guidance have relied on the biochemical nature of the cues delivered to the cell. We propose here that the physical characteristic, namely the resistance to displacement of the substrate, is an additional cue that cells can use to orient during migration.

Experimental Procedures

Cells, Reagents, and Microscopy

Experiments were performed on NIH 3T3 mouse fibroblasts transfected with the cDNA encoding the chick β1 subunit of integrin or a truncated subunit lacking the cytoplasmic tail (Hayashi et al., 1990). Cells were plated on laminin-coated, silanized glass coverslips (Schmidt et al., 1993) and visualized with a 1.3 NA 100×

plan–neofluar objective on an inverted microscope, Axiovert 100 TV, equipped with Nomarsky optics. The chamber and objective were maintained at 37°C by flowing heat–regulated air. Carboxylated latex beads (Polyscience, Warrington, PA) were coated with BSA or a given ratio of biotinylated to unbiotinylated BSA by use of a carbodiimide linkage (Kuo and Sheetz, 1993). Alternatively, unbiotinylated BSA–coated beads were then biotinylated with 60 μM NHS–LC–biotin (Pierce, Rockford, IL). The amount of FN7-10 per bead was varied in two ways: first, by varying the amount of biotin–BSA covalently linked on the beads and further incubating the latter with saturating concentration of avidin neutralite (Molecular Probes, Eugene, OR; 2 mg/ml, overnight at 4°C) then biotinylated FN7-10 (10–50 mg/ml; 1–3 hr at 22°C); second, by incubating maximally biotinylated beads with avidin neutralite (2 mg/ml), then with FN7-10 at decreasing concentrations (from 10 to 0.1 μg/ml). Identical categories of results were obtained with both methods (see Figure 2) and were pooled as follows. Category labeled control or none, biotinylated BSA was used instead of FN7-10 in the last binding step. Category low density, beads from the first method with 1%–3% biotinylated BSA as a first layer on the beads and beads from the second method incubated with 0.1 μg/ml FN7-10. Category medium density, beads from the first method with 5%–10% biotinylated BSA and beads from the second method incubated with 0.5 to 1.0 μg/ml FN7-10. Category high density, beads from the first method with 25%–100% biotinylated BSA and beads from the second method incubated with 10–50 μg/ml FN7-10. Bead incubations were performed at a bead concentration of approximately 2%. The number of bound FN7-10 molecules per bead was estimated by densitometry of dot blots of beads and standard amounts of FN7-10 and yielded numbers around 1000–5000 peptides per bead at high density. FN7-10 was detected with the mouse IST-6 anti-FN monoclonal antibody (Carnemolla et al., 1992) and an HRP sheep anti-mouse immunoglobulin (Amersham, Arlington, IL). The dot blot was then revealed by enhanced chemiluminescence. Anti-β1–coated beads were obtained by incubating overnight at 4°C carbodiimide-activated carboxylated latex beads (2% solution) with ES-66 anti-chick β1 antibody (Duband et al., 1988) at 500 μg/ml (high antibody coating) or 5 μg/ml (low antibody coating).

Optical Trapping and Data Analysis

Optical tweezers were set up and calibrated as described (Kuo and Sheetz, 1993). An Innova 70 argon laser pumped an 890 titanium-sapphire laser (Coherent, Bowie, MD) set at 800 nm. The intensity (0–1 watt) was varied linearly with a Polarcor polarizer (Newport, Irvine, CA). For tracking of the bead position and feedback on the piezoelectric stage, the outputs of a quadrant detector (Finer et al., 1994) receiving the bright-field image of the bead were fed to an analog circuit to give X and Y bead position. These were digitized at 4 KHz, numerically processed, and sent as output to the piezoelectric stage through a D/A board to maintain the bead in the center of the quadrant. Video frames were digitized and a single-particle tracking program used to detect bead position with a sensitivity of 5–10 nm for 1-μm beads (Gelles et al., 1988; Schmidt et al., 1993). A bead was considered as fixed on the cell surface for a given optical trap force when that force was unable to produce a detectable (i.e., $<$10 nm) movement of the bead. A bead was defined as movable when a clear rapid bead displacement above noise (about 25 nm) was measured on tracking plots within 100 ms of the application of the force.

Two-dimensional diffusion coefficient D and bead velocity V were computed by fitting the function $f(T) = 4DT + \beta T^2$ to the curve of mean squared displacement versus time as described by Qian et al. (1991). If β was negative or null, the track was said to be purely diffusive movement; otherwise, the velocity of directed displacement was taken as $V = \sqrt{\beta}$. We have performed χ^2 or Student's t statistical tests on the different sets of data.

Acknowledgments

Correspondence should be addressed to M. P. S. We thank H. P. Erickson for providing the recombinant FNIII-7-10 fragment, A. F. Horwitz for the 3T3 cell line, and R. Sterba for technical help. We thank H. P. Erickson, C. Galbraith, and C. Martenson for helpful comments on the manuscript. D. C. is a recipient of European Molecular Biology Organization, Fondation Cino, and Simone Del Duca fellowships. D. F. was supported by the Cancer Research Fellowship of the Damon Runyon-Walter Winchell Foundation. This work was supported by National Institutes of Health funds.

Received May 9, 1996; revised October 18, 1996.

References

Ashkin, A. (1992). Forces of a single-beam gradient laser trap on a dielectric sphere in the ray optics regime. Biophys. J. *61*, 569–582.

Carnemolla, B., Leprini, A., Allemanni, G., Saginati, M., and Zardi, L. (1992). The inclusion of the type III repeat ED-B in the fibronectin molecule generates conformational modifications that unmask a cryptic sequence. J. Biol. Chem. *267*, 24689–24692.

Crowley, E., and Horwitz, A.F. (1995). Tyrosine phosphorylation and cytoskeletal tension regulate the release of fibroblast adhesions. J. Cell Biol. *131*, 525–537.

Dalton, S.L., Marcantonio, E.E., and Assoian, R.K. (1992). Cell attachment controls fibronectin and alpha 5 beta 1 integrin levels in fibroblasts: implications for anchorage-dependent and -independent growth. J. Biol. Chem. *267*, 8186–8191.

Dembo, M., and Harris, A.K. (1981). Motion of particles adhering to the leading lamella of crawling cells. J. Cell Biol. *91*, 528–536.

Duband, J.L., Nuckolls, G.H., Ishihara, A., Hasegawa, T., Yamada, K.M., Thiery, J.P., and Jacobson, K. (1988). Fibronectin receptor exhibits high lateral mobility in embryonic locomoting cells but is immobile in focal contacts and fibrillar streaks in stationary cells. J. Cell Biol. *107*, 1385–1396.

Felsenfeld, D.P., Choquet, D.P., and Sheetz, M.P. (1996). Ligand binding regulates the directed movement of β1 integrins on fibroblasts. Nature *383*, 438–440.

Finer, J.T., Simmons, R.M., and Spudich, J.A. (1994). Single myosin molecule mechanics: piconewton forces and nanometre steps. Nature *368*, 113–119.

Forscher, P., and Smith, S.J. (1988). Actions of cytochalasins on the organization of actin filaments and microtubules in a neuronal growth cone. J. Cell Biol. *107*, 1505–1516.

Gelles, J., Schnapp, B.J., and Sheetz, M.P. (1988). Tracking kinesin-driven movements with nanometre-scale precision. Nature *331*, 450–453.

Halliday, N.L., and Tomasek, J.J. (1995). Mechanical properties of the extracellular matrix influence fibronectin fibril assembly *in vitro.* Exp. Cell Res. *217*, 109–117.

Harris, A.K., Stopak, D., and Wild, P. (1981). Fibroblast traction as a mechanism for collagen morphogenesis. Nature *290*, 249–251.

Hayashi, Y., Haimovich, B., Reszka, A., Boettiger, D., and Horwitz, A. (1990). Expression and function of chicken integrin beta 1 subunit and its cytoplasmic domain mutants in mouse NIH 3T3 cell. J. Cell Biol. *110*, 175–184.

Hynes, R.O., and Lander, A.D. (1992). Contact and adhesive specificities in the associations, migrations, and targeting of cells and axons. Cell *68*, 303–322.

Kimizuka, F., Ohdate, Y., Kawase, Y., Shimojo, T., Taguchi, Y., Hashino, K., Goto, S., Hashi, H., Kato, I., Sekiguchi, K., et al. (1991). Role of type III homology repeats in cell adhesive function within the cell-binding domain of fibronectin. J. Biol. Chem. *266*, 3045–3051.

Kucik, D.F., Kuo, S.C., Elson, E.L., and Sheetz, M.P. (1991). Preferential attachment of membrane glycoproteins to the cytoskeleton at the leading edge of lamella. J. Cell Biol. *114*, 1029–1036.

Kuo, S.C., and Sheetz, M.P. (1992). Optical tweezers in cell biology. Trends Cell Biol. *2*, 116–118.

Kuo, S.C., and Sheetz, M.P. (1993). Force of single kinesin molecules measured with optical tweezers. Science *260*, 232–234.

LaFlamme, S.E., Akiyama, S.K., and Yamada, K.M. (1992). Regulation of fibronectin receptor distribution. J. Cell Biol. *117*, 437–447.

Lauffenburger, D.A., and Horwitz, A.F. (1996). Cell migration: a physically integrated molecular process. Cell *84*, 359–369.

Leahy, D.J., Aukhil, I., and Erickson, H.P. (1996). 2.0 Å Crystal structure of a four-domain segment of human fibronectin encompassing the RGD loop and synergy region. Cell *84*, 155–164.

Lee, J., Leonard, M., Oliver, T., Ishihara, A., and Jacobson, K. (1994). Traction forces generated by locomoting keratocytes. J. Cell Biol. *127*, 1957–1964.

Lin, C.H., and Forscher, P. (1995). Growth cone advance is inversely proportional to retrograde F-actin flow. Neuron *14*, 763–771.

Lin, C.H., Espreafico, E.M., Mooseker, M.S., and Forscher, P. (1996). Myosin drives retrograde F-actin flow in neuronal growth cones. Neuron *16*, 769–782.

Lotz, M.M., Burdsal, C.A., Erickson, H.P., and McClay, D.R. (1989). Cell adhesion to fibronectin and tenascin: quantitative measurements of initial binding and subsequent strengthening response. J. Cell Biol. *109*, 1795–1805.

Mandeville, J.T. H., Lawson, M.A., and Maxfield, F.R. (1996). Dynamic imaging of neutrophil migration in three dimensions: mechanical interactions between cells and matrix. J. Leukoc. Biol., in press.

Mitchison, T.J., and Cramer, L.P. (1996). Actin-based cell motility and cell locomotion. Cell *84*, 371–379.

Miyamoto, S., Akiyama, S.K., and Yamada, K.M. (1995). Synergistic roles for receptor occupancy and aggregation in integrin transmembrane function. Science *267*, 883–885.

Oliver, T., Dembo, M., and Jacobson, K. (1995). Traction forces in locomoting cells. Cell Motil. Cytoskel. *31*, 225–240.

Qian, H., Sheetz, M.P., and Elson, E.L. (1991). Single particle tracking: analysis of diffusion and flow in two-dimensional systems. Biophys. J. *60*, 910–921.

Reszka, A.A., Hayashi, Y., and Horwitz, A.F. (1992). Identification of amino acid sequences in the integrin beta 1 cytoplasmic domain implicated in cytoskeletal association. J. Cell Biol. *117*, 1321–1330.

Romer, L.H., Burridge, K., and Turner, C.E. (1992). Signaling between the extracellular matrix and the cytoskeleton: tyrosine phosphorylation and focal adhesion assembly. Cold Spring Harbor Symp. Quant. Biol. *57*, 193–202.

Ruoslahti, E. (1988). Fibronectin and its receptors. Annu. Rev. Biochem. *57*, 375–413.

Sato, M., Levesque, M.J., and Nerem, R.M. (1987). Micropipette aspiration of cultured bovine aortic endothelial cells exposed to shear stress. Arteriosclerosis *7*, 276–286.

Schmidt, C.E., Horwitz, A.F., Lauffenburger, D.A., and Sheetz, M.P. (1993). Integrin–cytoskeletal interactions in migrating fibroblasts are dynamic, asymmetric, and regulated. J. Cell Biol. *123*, 977–991.

Sheetz, M.P. (1994). Cell migration by graded attachment to substrates and contraction. Semin. Cell Biol. *5*, 149–155.

Shirinsky, V.P., Antonov, A.S., Birukov, K.G., Sobolevsky, A.V., Romanov, Y.A., Kabaeva, N.V., Antonova, G.N., and Smirnov, V.N. (1989). Mechano-chemical control of human endothelium orientation and size. J. Cell Biol. *109*, 331–339.

Simmons, R.M., Finer, J.T., Chu, S., and Spudich, J.A. (1996). Quantitative measurements of force and displacement using an optical trap. Biophys. J. *70*, 1813–1822.

Sims, J.R., Karp, S., and Ingber, D.E. (1992). Altering the cellular mechanical force balance results in integrated changes in cell, cytoskeletal and nuclear shape. J. Cell Sci. *103*, 1215–1222.

Solowska, J., Guan, J.L., Marcantonio, E.E., Trevithick, J.E., Buck, C.A., and Hynes, R.O. (1989). Expression of normal and mutant avian integrin subunits in rodent cells. J. Cell Biol. *109*, 853–861.

Stopak, D., Wessells, N.K., and Harris, A.K. (1985). Morphogenetic rearrangement of injected collagen in developing chicken limb buds. Proc. Natl. Acad. Sci. USA *82*, 2804–2808.

Theriot, J.A., and Mitchison, T.J. (1991). Actin microfilament dynamics in locomoting cells. Nature *352*, 126–131.

Wang, N., and Ingber, D.E. (1994). Control of cytoskeletal mechanics by extracellular matrix, cell shape, and mechanical tension. Biophys. J. *66*, 2181–2189.

Wang, N., Butler, J.P., and Ingber, D.E. (1993). Mechanotransduction across the cell surface and through the cytoskeleton. Science *260*, 1124–1127.

Wessels, D., Soll, D.R., Knecht, D., Loomis, W.F., De Lozanne, A., and Spudich, J. (1988). Cell motility and chemotaxis in *Dictyostelium* amebae lacking myosin heavy chain. Dev. Biol. *128*, 164–177.

Zhelev, D.V., and Hochmuth, R.M. (1995). Mechanically stimulated cytoskeleton rearrangement and cortical contraction in human neutrophils. Biophys. J. *68*, 2004–2014.